



ELSEVIER

Atmospheric Research 62 (2002) 125–147

ATMOSPHERIC
RESEARCH

www.elsevier.com/locate/atmos

Convective available potential energy (CAPE) in Northern Africa and tropical Atlantic and study of its connections with rainfall in Central and West Africa during Summer 1985

David Monkam

Département de Physique, Faculté des Sciences, Université de Douala, B.P. 24 157 Douala, Cameroon

Received 3 May 2001; accepted 29 December 2001

Abstract

In this paper, we study the distribution of the convective available potential energy (CAPE) in northern Africa and tropical Atlantic in summer. The pattern of this parameter is quite steady and presents three main zones. The first one is located between the equator and 15°N – 20°N , with positive values of CAPE. In the second and the third zones located north of the band of latitudes 15°N – 20°N and south of the equator, respectively, CAPE has negative values. We examined, in some details, the main tendencies of the CAPE pattern inside the first zone (CAPE > 0 , in general) and we compared them to the rainfall pattern. We noted that the CAPE pattern in this zone presents three regions of maximum values: west, center, and east of the zone. The maximum at east and the maximum in the center seem to be connected to the orography effects. Between 15°N and 20°N , the CAPE distribution is characterised by its iso-line zero. This iso-line zero seems to define the north limit of the inter tropical convergence zone (ITCZ). In fact, the position of the iso-line zero on the CAPE distribution fluctuates during summer as the position of the ITCZ so that this parameter can also be used as a parameter or an index to define the ITCZ position in northern Africa and tropical Atlantic in the summer. The patterns of the rainfall and CAPE in this zone (5°N – 20°N) have a very good similarity. When the rainfall is very weak ($< 2 \text{ mm day}^{-1}$) towards 12.5°N – 15°N , the CAPE tends to become zero. The rainfall pattern presents, in general, high values towards Guinea and around Lake Chad. These regions are not very far from the maximum values of CAPE observed in different figures. The fields of correlation coefficients between the two parameters show that the rainfall and the CAPE are very well correlated around the ITCZ and towards some mountains. So, the strong values of the correlation coefficients seem to indicate that each of these two parameters is

E-mail address: monkam1@yahoo.fr (D. Monkam).

influenced by the ITCZ effects and by the orography effects. © 2002 Elsevier Science B.V. All rights reserved.

Keywords: Convective available potential energy (CAPE); Inter tropical convergence zone (ITCZ); Rainfall; Correlation; Coefficient; Orography

1. Introduction

The convection systems had been studied in some details, in the tropics and in the big American plains context in particular, using important means of equipments of observations and simulations. These studies had allowed to identify a certain number of mechanisms for convection: its initiation, its structural organisation, and its maintenance. About the initiation, an important investigation had been made by Balaji and Redelsperger (1996) who had studied the sub-gridscale effects in mesoscale deep convection in some details by examining different aspects: the initiation, the organisation, and the turbulence. Weisman and Klemp (1982) studied the dependency of numerically simulated convection storms on vertical wind shear and buoyancy. This study on the structural organisation of the convection took the problem of some instabilities into account, in particular, those that are related to the rising of the particle. Rotunno and Klemp (1982) examined the problem of the convection maintenance when investigating the influence of shear-induced pressure gradient on the thunderstorms motion.

However, three fundamental principles rule over the convection or must be taken into account when studying the convection phenomena: the first one concerns the instability; the second, the rising; and the last one, the humidity feeding.

The instability is a necessary condition for convection and had instigated an important interest. Therefore, many studies had been done about the subject. Showalter (1953) introduced an index to indicate or characterise the instability. Some other studies also tend to take into account the instability as an index. So, there is a variety of propositions about the definitions of the instability index and many authors have shown that the pertinence of the choice of this index for the prevision of convection or the prevision of quantities of the associated precipitation could be variable according to the locality. However, the problem of defining or creating an index must be treated with some precautions. In fact, when we looked on the specialised different references concerning the convection, we inventoried more than 60 indices or parameters about instability or convection systems.

However, a certain number of definitions of instability indices had been given (Peppler and Lamb, 1989). According to some recent studies, the instability indices can be classified into three main groups. The first one concerns the parameters or indices linked to the theory of the rising of the particle; the second is for parameters linked to the releasing by the diurnal heating; and the last one is obtained from different arrangements between some indices, in particular after some numerical treatments.

Now, in this general context, we examined the case of northern Africa, and it seems that for our study in the mesoscale in this region, particularly during summer, the deep convection may be among the most important convection systems. We examined the convection based on the theory of the rising of the particle, implying the energy of ascension. The

convective available potential energy (CAPE), defined as an instability or convection index, contributes to this energy. In fact, the CAPE looks more simply like the part of the particle potential energy that is necessary to condense when thermodynamical conditions are fulfilled.

From what we have said above, some thermodynamical aspects of the moisture atmosphere evolution must be rapidly recalled. A connection may exist between Equivalent Potential Temperature (EPT) and rainfall, and, on the other hand, a relation between CAPE and rainfall which is one of the main results of the convection which can be expected, in particular, over continental regions of the studied area, during summer.

So, our aim in the present work is to study the distribution of CAPE and examine the eventual connections with some phenomena of this region. In particular, we want to make some investigations, in a comparative study, of CAPE and rainfall during summer, a period corresponding to the rainy season in the Sahel region. So, we expect that the rain data will not be very erratic in this zone of northern Africa, particularly in Central and West Africa. In the next section, we describe the data that were used and those that were present in the studied area. In Section 3, we describe the method that was used to compute CAPE, while in Section 4, we study the variability of CAPE in the studied area during the summer of 1985. In Section 5, we study the steadiness of the CAPE pattern during summer, with the climatology of the Central and West Africa. In Section 6, a comparative study between CAPE and rainfall is made. In Section 7, we discuss the different results in connection with some features of the area of study.

2. Data

We used data coming from the National Center for Environmental Prediction (NCEP) and the National Center for Atmospheric Research (NCAR). NCEP and NCAR have completed a reanalysis project with a current version of the Medium Range Forecast (MRF) model. This dataset consists of a reanalysis of global observational network of meteorological variables like wind, temperature, geopotential height or pressure level, humidity, surface variables, and flux variables like precipitation rates, with a “frozen” state-of-the-art analysis and forecast system at a triangular spectral truncation of T62 to perform the data assimilation throughout the period 1958 to the present. This enables us to circumvent problems of previous numerical weather prediction analyses due to changes in techniques, models, and data assimilation. Data are reported on a $2.5^\circ \times 2.5^\circ$ grid every 6 h (0000, 0600, 1200, and 1800 UTC) in 17 pressure levels from 1000 to 10 hPa which are good resolutions for studies of middle scale. To compute the CAPE, we used the data for the levels 1000, 925, 850, 700, 600, 500, 400, 300, 250, and 200 hPa. We worked with the data for the 1 June to 30 September period. We selected the NCEP/NCAR data on the area bounded by the latitudes 10°S and 30°N and the longitudes 30°E and 30°W .

About the rain data, daily rainfall dataset had been compiled by the Institut de Recherche pour le Developpement (IRD, previously called ORSTOM). The compilation consists of about 1000 stations located in the domain 5°N – 22°N and 17.5°W – 22.5°E . The daily values have been interpolated in space on the NCEP $2.5^\circ \times 2.5^\circ$ grid by assigning a daily value to the nearest grid point for each station and by averaging all the values related to each

grid point. They have also been interpolated in time, related to NCEP daily wind fields, since daily rainfall amounts were measured between 0600 UTC of the day and 0600 UTC of the following day. So, we had homogenous daily rainfall data on which semidiurnal and phenomena of the period under a day are removed. In fact, these phenomena can have some influences on data series; Duvel (1989), studying convection over tropical Africa and the Atlantic ocean during northern summer, indicates a maximum of high cloud coverage over land between 1800 and 0000 UTC. Sow (1997), studying diurnal rainfall variations in Senegal, notes a maximum of precipitation between 1700 UTC at the end of the night.

So, we finally obtained daily rainfall values from 1 June to 30 September (122 values). For any investigation, taking the rainfall data into account, we limited the study to the domain where the two quantities, rainfall and NCEP data, are available together. Therefore, the studied area for the comparison between CAPE and rainfall is defined by 5°N – 20°N , 17.5°W – 22.5°E . To have homogenous data for both CAPE and rainfall series, since we had daily values for rainfall, we also computed the daily CAPE by averaging the four outputs of each day for the NCEP/NCAR data. The rainfall data are also available on the NCEP/NCAR reanalyses. Fontaine et al. (1999) compared the rainfall in West Africa given by the NCEP/NCAR system to the observed rainfall indices. Correlation coefficients between reanalyses precipitation and rain gauge-based indices, computed for the time interval 1968–1994, are around 0.74 for July–September for the Guinea coast index, and only 0.34 for the Sahel index. So, a problem of non-homogeneity for these NCEP/NCAR precipitation reanalyses seems to exist. We did not use the NCEP/NCAR rainfall reanalyses data, though we used specific humidity given by this system. In fact, it seems that the problem of the Sahel result is due to a very important decrease of NCEP/NCAR rainfall for this period of 1968–1994.

3. Convection and cape computation

Observations indicate that most of the precipitations in the tropical systems are of convective origin. Mesoscale storms that are associated with very deep vigorous cumulus convection must be taken into account. So, the nature of the interaction between the cumulus scale motions and the synoptic scale disturbances in which the cumulus motions are embedded must therefore be elucidated. However, convective motions are generally non-hydrostatic, non-steady turbulent motions that require the full three-dimensional equations of motion for their description. One of the important aspects of the moist convection concerns the thermodynamic, particularly when vertical motion is considered.

The convective available potential energy (CAPE) is an index, among several others, to measure the susceptibility of a given temperature and profile to the occurrence of deep convection. In fact, convection over continental regions (such as tropical Africa) can be initiated without significant boundary layer convergence, since strong surface heating can produce positive parcel buoyancy all the way to the surface. However, sustained deep convection requires mean low-level moisture convergence, and the development of convective storms depends on the presence of environmental conditions that are favourable for the occurrence of deep convection. The convective available potential energy can be a useful measure of the maximum possible kinetic energy that a statically unstable parcel can require, assuming that the parcel ascends without mixing with the environment, and

instantaneously, adjusts to the local environmental pressure. Finally, CAPE measures when thermodynamic conditions are favourable for the development of cumulus convection, and, therefore, provides a guide to the strength of convection.

CAPE is an instability index that is related to the theory of up thrust. It is a measurement of the kinetic energy that a buoyant parcel could obtain by ascending from a state of rest at the level of free convection (LFC) to the level of neutral buoyancy (LNB) as we said above. The kinetic energy for a parcel of unit mass, going vertically, is given by $(w^2/2)$, where w is the vertical component of the velocity. Holton (1992) indicated that CAPE corresponds to the maximum value of $(w^2/2)$, which is $(w_{\max}^2/2)$, where w_{\max} is the maximum value of w so that we can write:

$$\text{CAPE} = w_{\max}^2/2 = \int_{Z_{\text{LFC}}}^{Z_{\text{LNB}}} g \left(\frac{T_{\text{parcel}} - T_{\text{env}}}{T_{\text{env}}} \right) dz \quad (1)$$

where T_{parcel} designates the temperature of the parcel and T_{env} , the temperature of the environment. Z_{LFC} designates the level of free convection and Z_{LNB} , the level of neutral buoyancy. Considering the atmosphere as an ideal gas in a hydrostatic equilibrium, assuming T_{parcel} to be the virtual temperature T_v and T_{env} to be the mean value of T_v noted \bar{T}_v , the relation (1) becomes:

$$\text{CAPE} = \int_{P_{\text{LFC}}}^{P_{\text{TOP}}} ((T_v - \bar{T}_v) R_a d(\text{Log}P)) \quad (2)$$

Expression (2) is the one given by Moncrieff and Miller (1976) to compute the convective available potential energy.

P_{LFC} designates the pressure level from which the buoyancy becomes positive (Fig. 1). It is the level of intersection between the state curve of sounding and the saturated adiabatic curve, reached by a parcel, which, from the ground level, ascended, following the dry adiabatic until the pressure level P_{LCL} , called the lifting condensation level, and then eventually continues to go up following pseudo-adiabatic curve.

In fact, when a parcel ascends from the ground level, following dry adiabatic, it can eventually become saturated at the lifting condensation level (LCL). If that parcel continues to rise, it will follow the pseudo-adiabatic and it will reach a level at which it becomes buoyant, relative to its surroundings, and can then freely accelerate upward; this occurs at the level of free convection (LFC).

P_{TOP} is the pressure of thermic equilibrium, corresponding to the top of the CAPE zone. At P_{TOP} , the pseudo-adiabatic curve again meets the curve of state of the particle, as shown on Fig. 1. The zone corresponding to the CAPE is clearly indicated in this figure. The CAPE is the surface between the pseudo-adiabatic curve and the state curve followed by the parcel. In the practical point of view, we computed this surface using the trapezoid method of integration with the following considerations:

P_{LFC} is fixed at 700 hPa level and

P_{TOP} is fixed at 200 hPa level.

At each grid point, a numerical approach of the variation of the virtual temperature of the pseudo-adiabatic curve (T_{v_psad}) in function of pressure levels is computed; this is the

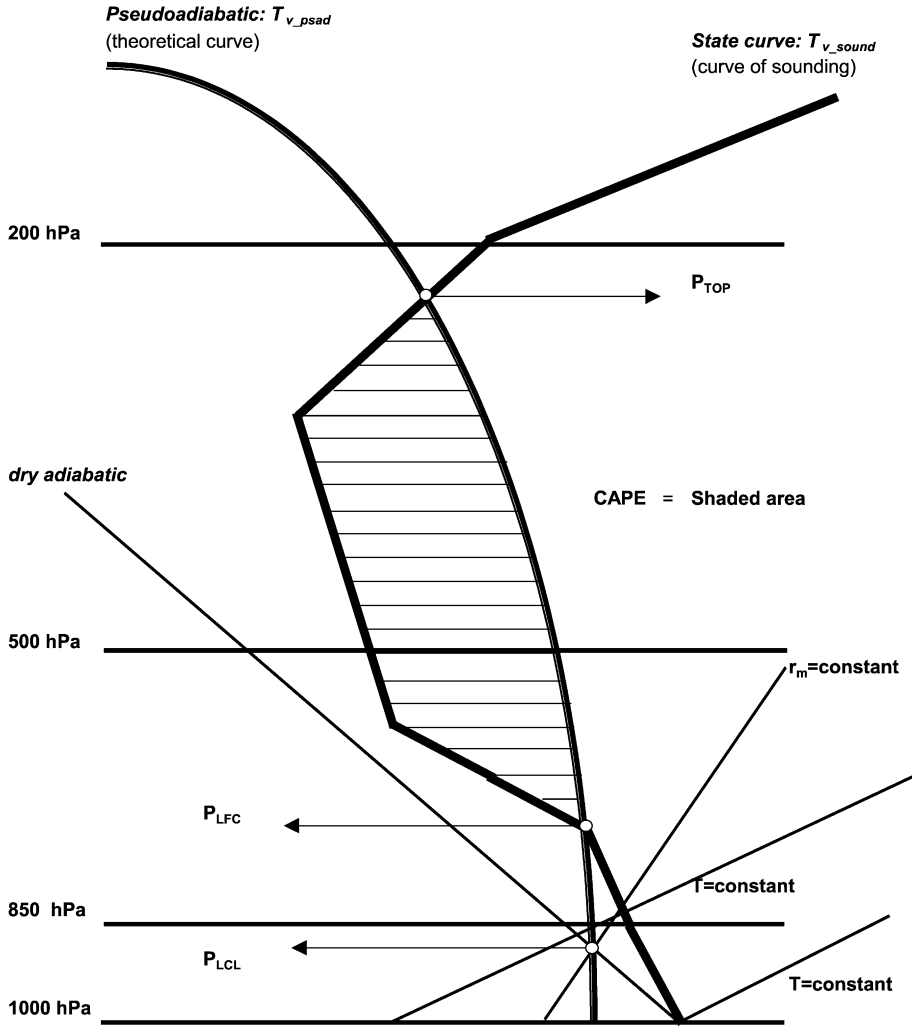


Fig. 1. Schematic illustration of CAPE: the shaded area.

numerical theoretical curve of the particle evolution. At each grid point, from the data of temperature and specific humidity given at different pressure levels, we computed the virtual temperatures of the curve of sounding (T_{v_sound}); this is the numerical state curve of the particle. So, using the trapezoid numerical method of integration, we computed the area between the two curves of temperatures between the pressure levels 700 and 200 hPa for each grid point of the studied area. The relation (3) that was used is written below:

$$\begin{aligned}
 \text{CAPE} = & \frac{1}{2} \sum_{k=11}^{k=12} [(T_{v_psad}(k+1) - T_{v_sound}(k+1)) + (T_{v_psad}(k) - T_{v_sound}(K))] \\
 & \times [P(k) - P(k+1)].
 \end{aligned}
 \tag{3}$$

- k number of the level, from l_1 to l_2
 l_1 number of the low level
 l_2 number of the high level

As we indicated in Section 2, when we described the data used, we had 10 levels from 1000 to 200 hPa, corresponding to level numbers 1 and 10, respectively. To compute CAPE, we fixed P_{LFC} at 700 hPa (level number 4) and P_{TOP} at 200 hPa (level number 10).

Looking into the relation (1), given by Holton (1992), the CAPE can be given in $\text{m}^2 \text{s}^{-2}$ or in J/kg (as an energy). Considering the expression (3) that was used in practice, we see that the CAPE can also be given in $P_a K$ (for pressure and temperature). So, these different units designate the same quantity or parameter. Therefore, in the text below, any one of them will be indifferently used.

4. Description of the cape in the studied area

To examine in some details the variability of CAPE, we first show a general view of the distribution of this quantity in the studied area. So, we present on Fig. 2, the seasonal field of the CAPE corresponding to the mean field for summer. In fact, this period (1 June to 30 September) corresponds to the rainy season in the Sahel, during which problems of convection or deep convection, rainfall, and many other features in connection with convective activities have more effects or are more identified. Fig. 2 displays the mean values of CAPE computed for the whole summer in the studied area. In this figure, three main zones appear. The first one is located between the equator and the latitude 15°N , with positive values of CAPE in general. In this zone, the mean CAPE maximum values around $2000 \text{ m}^2 \text{ s}^{-2}$ are observed at the east, center, and west parts of the zone. In the other parts of this zone,

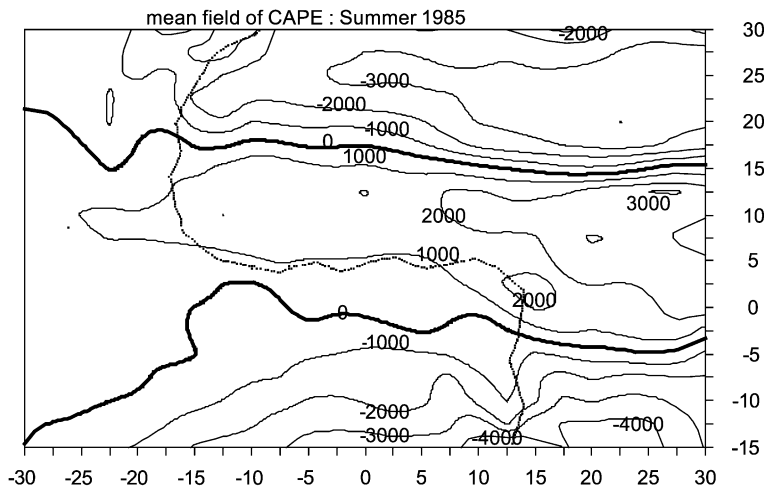


Fig. 2. Mean field of CAPE for Summer 1985. Abscissa: longitudes in degrees, ordinate: latitudes in degrees.

values are, in general, under $1000 \text{ m}^2 \text{ s}^{-2}$. The second region appearing in the field extends from about 15°N to 30°N , with negative values of CAPE; in the second zone, at east of the Greenwich meridian, the negative values are strong, around -3500 or $-3000 \text{ m}^2 \text{ s}^{-2}$, while west of the Greenwich meridian CAPE is around $-500 \text{ m}^2 \text{ s}^{-2}$. The third zone that we distinguish on Fig. 2 is situated south of the equator, with also negative CAPE in general as in the second zone, in particular at the east of the longitude 20°W .

As a whole, Fig. 2 shows that in the studied area, the north of the latitude 15°N and the south of the equator are two zones of important deficit of energy which must be filled by means of different mechanisms of the atmospheric energy transfer, transport, or exchange. Charney (1975), studying the dynamics of deserts and drought in the Sahel, also noted this important deficit of energy. This author made some investigations and gave some explanations about the energy deficit that was observed in the Sahara desert in particular, and for other dry regions of the globe in general, and also suggested the mechanisms filling the energy deficit in those regions. We shall deal with the problem of energy exchange later, but we can already note that the CAPE seasonal-scale distribution allows to observe the zones which can be considered as a source or as a sink of energy in northern Africa and tropical Atlantic during summer.

The zone of positive values of CAPE observed between the equator and 15°N contains the band of latitudes inside which is the inter tropical convergence zone (ITCZ) location during summer in northern Africa. Many studies agree that the ITCZ oscillates into the band of latitudes 5°N – 15°N during this period. So, this zone of positive CAPE seems to be connected to the ITCZ and also to the meridional extension of the monsoon layer in this period of the year in Central and West Africa. It is clearly known that the summer monsoon meridional extension is strongly related to the ITCZ.

This zone of positive CAPE can be separated into three bands of longitudes of local maximum: the first one (see Fig. 2) is at the east part of the studied area, between 27.5°E and 22.5°E towards the latitude 12.5°N , with a mean value around $3000 \text{ m}^2 \text{ s}^{-2}$. The second zone of maximum CAPE is located towards the Greenwich meridian for the same latitude but with a mean value of about $2000 \text{ m}^2 \text{ s}^{-2}$. The last one is located around the meridian 12.5°W and the parallel 10°N with a mean of $2000 \text{ m}^2 \text{ s}^{-2}$. At the west of this meridian 12.5°W , the CAPE is weak, with values under $1000 \text{ m}^2 \text{ s}^{-2}$ in general.

We note that the zones of maximum values of CAPE that are presented are not very far from some mountains above 1500 m, in particular for the maximum at the east and the maximum towards the center of the figure. We shall deal with this aspect later, after the examination of the steadiness of the structure that was observed. So, we computed the monthly mean values (June, July, August, and September) and the decadal mean values (12 decades during summer). Below, we briefly present some of the obtained results for these mean fields.

5. Steadiness of cape pattern over northern Africa and tropical Atlantic

Fig. 3a–d show the mean CAPE for June, July, August, and September, respectively. In June (Fig. 3a), the pattern is quite similar to what we obtained for the whole summer. The three bands of latitudes of negative, positive, and negative values of CAPE from north to

south of the studied area, or vice versa, are systematically reproduced in June; the three bands of longitudes (or the meridian) of local maximum in the zone of positive CAPE (between equator and 14°N – 15°N) are also visible; the values for these three zones of maximum are around $2000\text{ m}^2\text{ s}^{-2}$. In July (Fig. 3b), the zone of positive CAPE seems to be larger than in June. The CAPE mean values are, in general, stronger than in June in this positive zone, and the three bands of longitudes of local maximum extend spatially with a mean value around $3500\text{ m}^2\text{ s}^{-2}$ for the eastern one. The pattern obtained in August (Fig. 3c) is very close to the July month, while in September (Fig. 3d), the values are slightly

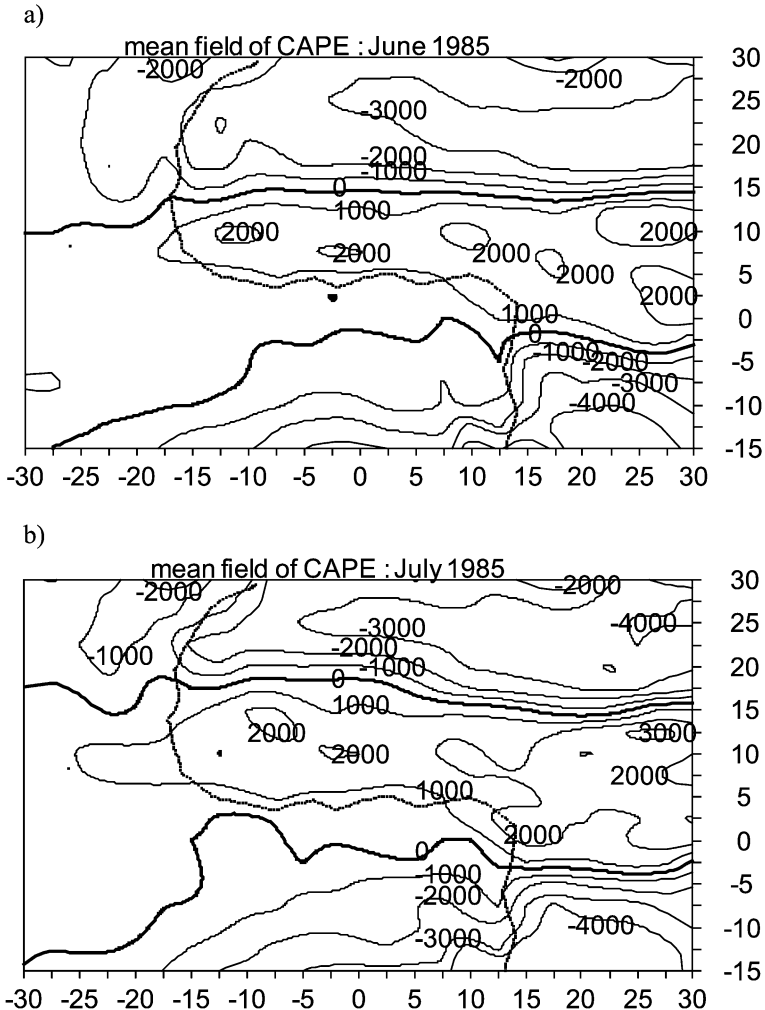


Fig. 3. Monthly fields of CAPE in 1985: (a) June, (b) July, (c) August, (d) September. Abscissa: longitudes in degrees, ordinate: latitudes in degrees.

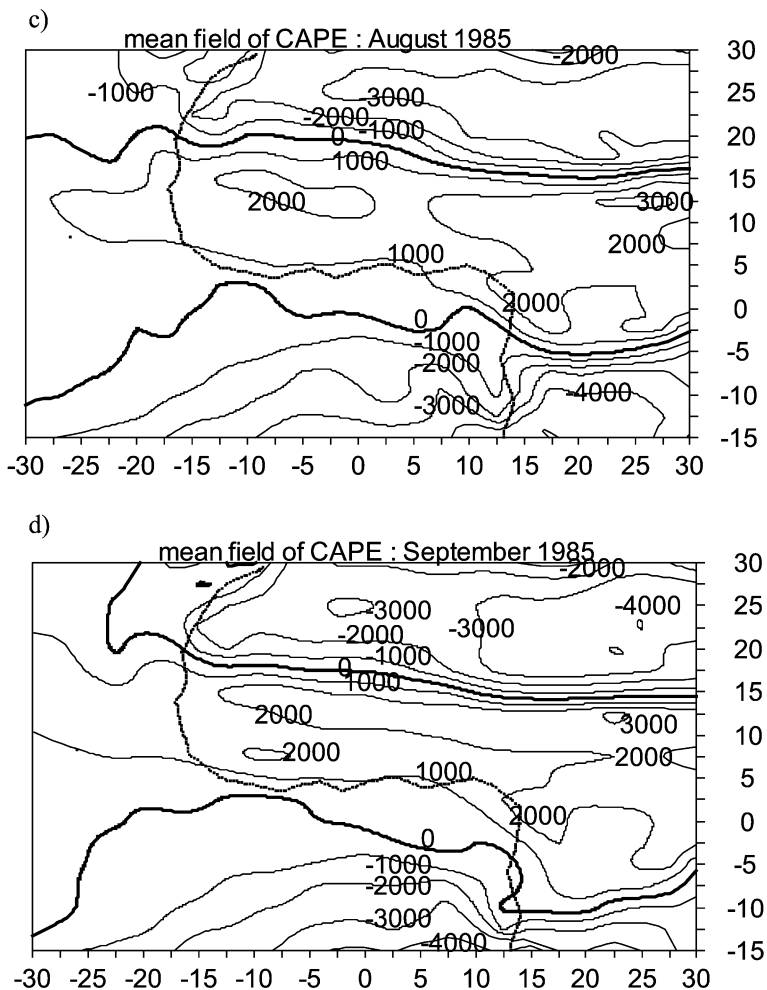


Fig. 3 (continued).

smaller than for the two previous months; the zone of positive CAPE extends more towards the south of the equator.

Finally, we note that the pattern of CAPE that was observed in the seasonal field is maintained on the menstrual fields; this shows the stability of the parameter CAPE with seasonal and menstrual time scales. Even inside the zone of positive CAPE, in mean, between the equator and 14°N – 16°N , the three zones of maximum are systematically permanent. To examine the case of short time scales, we briefly present the results obtained for the decadal fields. We computed the CAPE for the 12 decades of summer (not shown). We noted that as a whole, the steadiness of the pattern that was observed on seasonal and menstrual fields is systematically maintained on decadal mean fields. For the first decade (1 to 10 June) and the last decade (19 to 30 September), the zone of positive

CAPE extends more in the south of the equator. In fact, these decades correspond to the beginning (decade 1) and the end (decade 12) of the summer; nevertheless, the main tendency of the CAPE pattern remains unchanged in the zone of our interest, in the north of the equator, even on these two decades.

Through seasonal, menstrual, and decadal mean fields of CAPE, we see that the pattern is steady and permanent during summer in northern Africa. In this period, the band of latitudes that is relative to the ITCZ location seems to be well determined by the iso-line of $CAPE = 0$, between 5°N and 15°N at the north limit of the zone of positive CAPE. We also note that the ITCZ does not move inside the zone of negative values of CAPE during summer in northern Africa. It is also in this domain of positive CAPE that an important part of the convection affecting some features of northern Africa and tropical Atlantic north are generally identified. So, the oscillations, as easterly waves, commonly called African waves, and the 6–9-day waves, had been generally said to have important convective activities. Many studies about these oscillations, in connection with convection, had been done by different authors. For the easterly waves, we can note, for example, Reed et al. (1977, 1988), Duvel (1990), Monkam (1990), de Felice et al. (1990), Cadet and Houston (1984), Cadet and Nnoli (1987), Viltard et al. (1998), who investigated about convective activities in connection with the phenomena of the 6–9-day period in the band of latitudes 5°N – 20°N . In any case, these authors used different types of data and applied different methods, but they obtained their good results on this area of positive CAPE. Therefore, a connection between CAPE and rainfall can be expected in this region.

6. Cape and rainfall in Central and West Africa

We recall that in view of comparing the CAPE pattern and the rainfall pattern in Summer 1985, we consider the domain where the two quantities CAPE and rainfall are available together. This domain is limited by the band of latitudes 5°N – 20°N and longitudes 17.5°W – 22.5°E . To have a homogenous data series for CAPE and rainfall, since we had daily values for rainfall, we computed the daily CAPE by averaging the four values of CAPE determined from the four outputs of the NCEP/NCAR data. We described the variability of the rainfall and the CAPE in this area, we compared their patterns, and we presented the results for the fields of correlation between the two parameters.

6.1. Variability of rainfall

For the evolution of the rainfall during Summer 1985, we established mean fields of rainfall in June, July, August, and September 1985. In June, as can be seen in Fig. 4a, the mean rainfall pattern consists of about 5 – 6 mm day^{-1} of maximum inside the band of latitudes 7°N – 10°N , while in the north of 12°N , the values are weak, smaller than 2 mm day^{-1} . We also note that towards the grid points (5°N – 7.5°W) and (5°N – 5°W), in the south–west part of the zone, near Abidjan in Ivory Coast, the rainfall mean value in June is greater than 10 mm day^{-1} , with a maximum of around 12 mm day^{-1} . In a general point of view, the field of rainfall in June divides the zone into two parts: one south of the latitude 10°N where rainfall amount is strong, and another one north of 10°N where

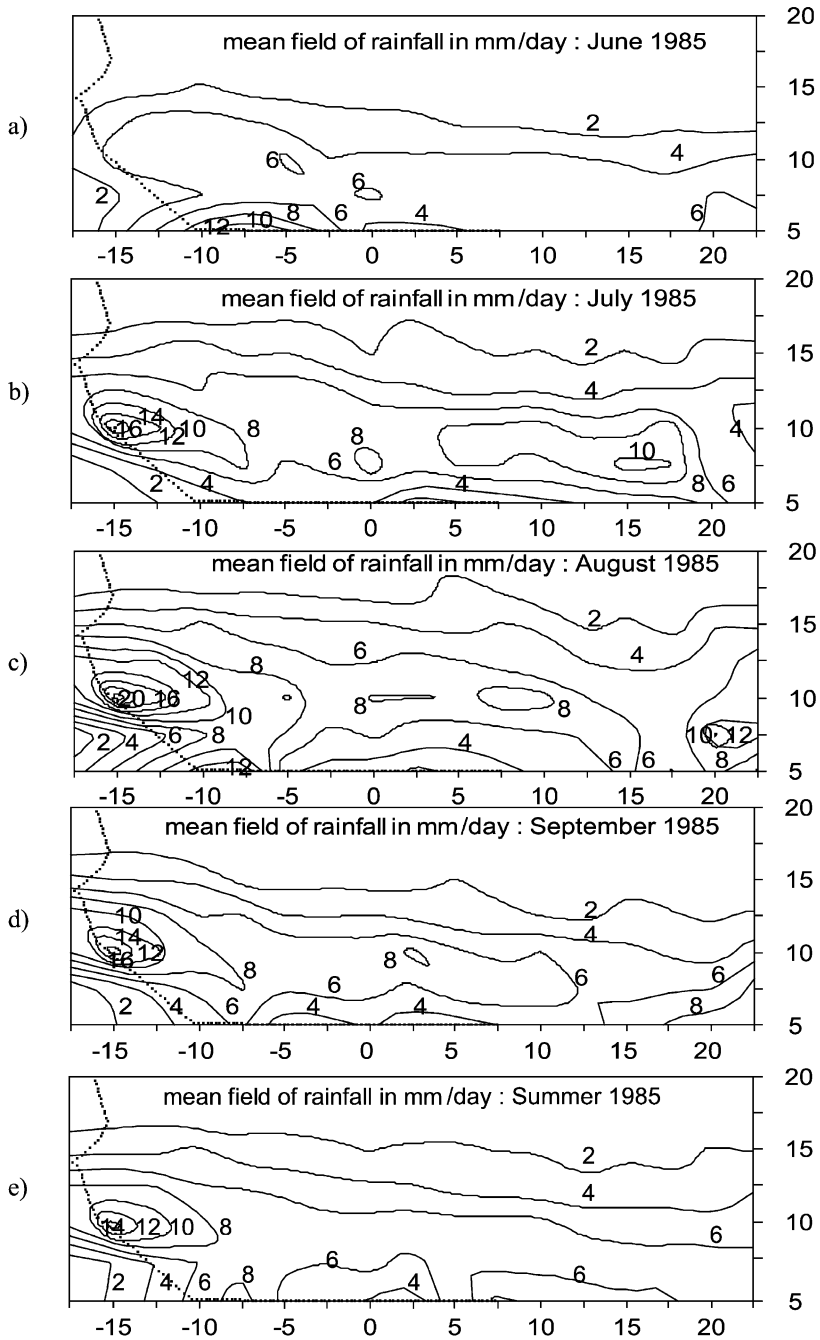


Fig. 4. Mean fields of rainfall in mm day⁻¹: menstrual and seasonal for Summer 1985; longitude (abscissa), latitude (ordinate) in degrees.

rainfall mean value is very weak. This may indicate that in June, the ITCZ location is slightly in the south (south of 10°N), particularly in the west part of the African continent.

In July, as can be seen in Fig. 4b, the values are greater than in June, with maximum of about $9\text{--}16\text{ mm day}^{-1}$ towards 10°N . In the band of latitudes $7^{\circ}\text{N}\text{--}12^{\circ}\text{N}$, values are, in general, greater than 7 mm day^{-1} . In the west part of the area, an important maximum of around 16 mm day^{-1} is observed towards Guinea, south of Senegal. This maximum is probably in connection with the Fouta-Djallon, with its main part located in Guinea-Bissau. Another maximum of about 10 mm day^{-1} is observed in the east of Cameroon and the west of Central African Republic. This region seems to be submitted in some way to the influences of the Ethiopian mountains in the lower levels. We note that for the month of July, as a whole, rainfall increases and the location position of the ITCZ is slightly in the north, towards $12^{\circ}\text{N}\text{--}15^{\circ}\text{N}$, comparative to the June month, everywhere in the studied area.

In August (Fig. 4c), the situation is close to what we have observed in July. The maximum value is greater than in July, about 20 mm day^{-1} towards Guinea around ($10^{\circ}\text{N}\text{--}15^{\circ}\text{W}$), and another one of about 12 mm day^{-1} towards the south of Lake Chad in the same regions as in July. In general, the rainfall mean values in August are greater than in July in the whole studied area. As a whole, the ITCZ had moved slightly to the north near 15°N . Towards this latitude, the mean rainfall is not as weak as in July and mainly in June, around 6 mm day^{-1} in the west part of the zone. We can note that during the month of August, the rainfall mean value reaches 3 mm day^{-1} at the latitude 17.5°N .

In September (Fig. 4d), rainfall mean values are decreasing; the maximum is around 17 mm day^{-1} towards ($10^{\circ}\text{N}\text{--}15^{\circ}\text{W}$), in the same region as in July and August. At the north of 15°N , the rainfall mean values are under 2 mm day^{-1} . The ITCZ location is slightly in the south, towards 12.5°N , as compared to August. Finally, among the 4 months of the summer, July and August are the two main months of strong rainfall amount. The ITCZ moves more to the north as compared to the two other months, June and September. Fig. 4a–d show that in July and August, the ITCZ is located at its most northern position over West Africa in the northern summer during the rainy season in Sahel.

Considering the mean field of rainfall during the whole summer, as shown on Fig. 4e, we note that the mean rainfall pattern during this period consists of a rainbelt of about $6\text{--}8\text{ mm day}^{-1}$ at $7.5^{\circ}\text{N}\text{--}12.5^{\circ}\text{N}$, up to more than 14 mm day^{-1} towards the Fouta Djallon mountains, with a rapid rainfall decrease northward leading to a mean amount of about $2\text{--}3\text{ mm day}^{-1}$ towards 15°N . At the south of Lake Chad, the maximum value is around 7 mm day^{-1} . Finally, as a whole, what we observed about the rainfall mean field and evolution during Summer 1985 is in agreement with the general tendency that is known in the studied area at this period of the year, in particular, the deep convection in the ITCZ at about $7^{\circ}\text{N}\text{--}12^{\circ}\text{N}$ during the summer, as we described in some details.

6.2. Variability of CAPE

Fig. 5a–d show the mean CAPE in the domain $5^{\circ}\text{N}\text{--}20^{\circ}\text{N}$, $17.5^{\circ}\text{W}\text{--}22.5^{\circ}\text{E}$, respectively for June, July, August, and September. In June (Fig. 5a), CAPE is positive at south of 12.5°N and negative at the north. In the south, there are four regions of

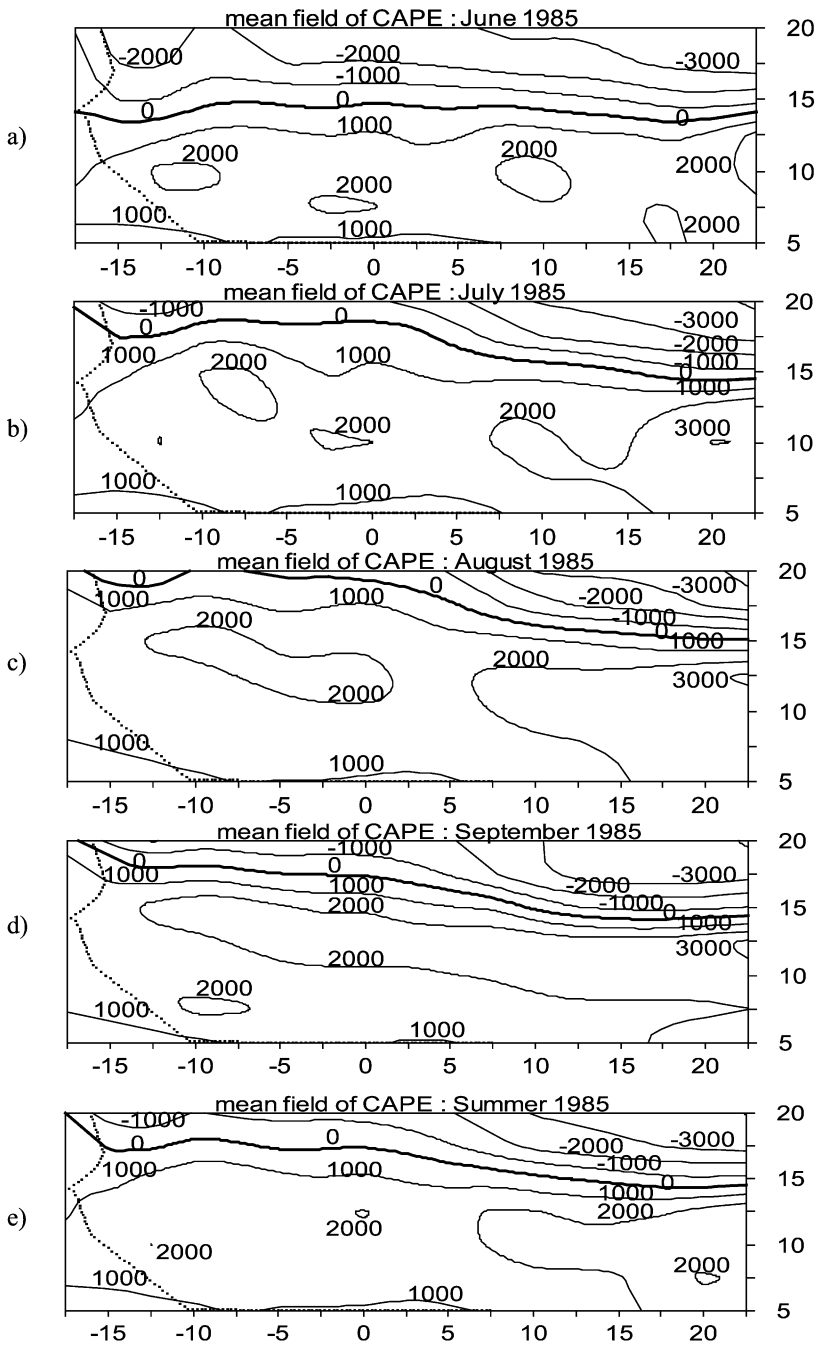


Fig. 5. Mean fields of CAPE: menstrual and seasonal for summer 1985; longitude (abscissa), latitude (ordinate) in degrees.

maximum (CAPE ≥ 2000), at the east, towards Lake Chad, near Greenwich meridian, and at the west towards Guinea. In July (Fig. 5b), the line corresponding to CAPE = 0 moves to the north, around 15°N in the east, and about 17.5°N in the center and west of the area. The zones of maximum observed in June are maintained, and CAPE values are amplified. The pattern in August (Fig. 5c) is very close to July though the line zero of CAPE moves slightly more to the north, around 15°N at east and near 20°N towards center and west of the area. CAPE values are more amplified than in July. In September (Fig. 5d) the line of CAPE = 0, moves to the south.

Finally, the CAPE pattern in the area systematically defines the northern limit position of the ITCZ during summer. This limit is clearly shown every month with the maximum northern position in July and August. The pattern observed during the four months is maintained in the seasonal mean field (Fig. 5e) with the iso-line zero occupying a mean position between 12.5°N and 15°N . So, the CAPE pattern is very steady. Even inside the zone of positive CAPE between the equator and 14°N – 16°N , the three zones of maximum are systematically permanent.

The ITCZ location, seems to be well determined by the iso-line zero of CAPE, between 5°N and 15°N , using CAPE pattern.

6.3. Comparison between CAPE and rainfall patterns

The rainfall pattern as presented on the mean field for summer and on the monthly fields is characterised by three main aspects:

- The first one is that the iso-lines of rainfall are zonal and the values decrease from south to north in general.
- The zone of strong values is limited by the band of latitudes 7°N – 12°N with a permanent maximum varying during summer from 12 to 20 mm day^{-1} around the meridians 14°W – 16°W , towards the Fouta-Djallon mountains in Guinea-Bissau. Another permanent maximum but not bigger than the first one is observed south of the Lake Chad with rainfall value varying from about 6 to 10 mm day^{-1} during summer.
- The third important feature of the rainfall pattern observed in summer is that north of a latitude in 12°N – 16°N , rainfall is very weak, tends to zero. On this last aspect of the rainfall pattern, there is a very good similarity with the CAPE pattern.

For the CAPE pattern, two or three main aspects can be retained:

- The first one is the separation of the area into two parts, one south of 15°N – 16°N with positive values and the second one north of 15°N – 16°N with negative values. The iso-line zero separating the two parts is inside the band of latitudes 15°N – 16°N and must be compared to the iso-line of very weak rainfall ($\leq 2 \text{ mm day}^{-1}$) appearing in the band 12°N – 15°N (Fig. 4a–e). These two lines (the line zero of CAPE and the line of weak rainfall) define or lay out each one, the northern limit of the ITCZ, and allow to indicate the horizontal width of the summer monsoon in this area.
- The iso-lines of CAPE also show two or three zones of maximum in the band of latitudes 7°N – 12°N , one towards Lake Chad, the second near Greenwich meridian and the third one around Guinea Bissau. These tendencies also appear on the rainfall pattern as we described above, though they are not predominant. To examine the connection between

rainfall and the CAPE in some details, we present below the fields of correlation coefficients computed between the two parameters.

6.4. Fields of correlation coefficients between cape and rainfall

We recall that before the computation of coefficients of correlation we applied a high pass filter centered in the frequency 0.00 day^{-1} on data series to remove trends. Therefore the coefficients of correlation obtained are not very large as for those computed with data series containing trends. But we recall that after high pass filter application on different time series, each coefficient of correlation r equal or greater than 0.2 ($r \geq 0.2$) is significant at least at 95%. We computed correlation between CAPE and rainfall in different grid points of the zone defined above in different cases.

We computed coefficients of correlation with a time-lag of 1 to 14 days between series of CAPE and rainfall. The series of CAPE are put back to 1 to 14 days. From time-lag of 2 to 14 days, coefficients of correlation were, in general, very weak (not shown). We show only the fields obtained with a time-lag of 1 day and without time-lag, on Fig. 6a and b, respectively. On Fig. 6a, the coefficients greater than 0.2 or equal to 0.2 are in general north of 12.5°N , in three main regions: the first one appears in the band of longitudes $22.5^\circ\text{E} - 17.5^\circ\text{E}$, north of the Lake Chad and just south of the Tibesti mountains ($r = 0.36$); the second region is located between the meridian 7.5°E and the Greenwich meridian, between Niger and Mali, and south of the Hoggar mountains ($r = 0.38$); the third region of

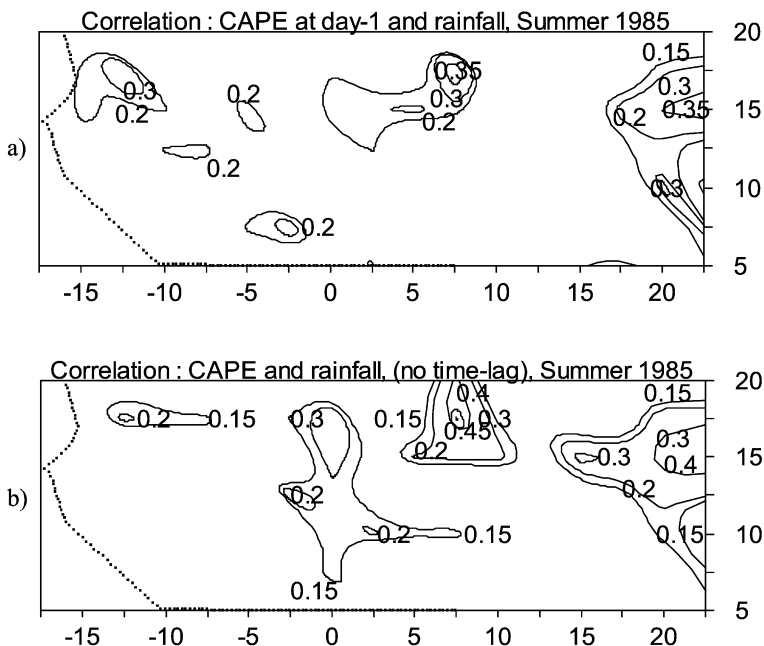


Fig. 6. Correlation between CAPE and rainfall for Summer 1985; longitude (abscissa), latitude (ordinate) in degrees.

significant r is towards Mauritania and Senegal, between longitudes 10°W and 15°W ($r=0.30$). Looking for the Fig. 6b, the pattern is not very different but the regions of significant r are larger than on Fig. 6a, r reaches the maximum values of 0.40, 0.45, and 0.22 at the grid points (15°N , 20°E), (17.5°N , 7.5°E), and (15°N , 12.5°W), respectively.

From these two figures, it seems that they are strongly connected to the topography of the area. The greatest coefficients of correlation appear near the mountains, in particular at the east and the central part of the area. We can even note that the zone where r is significant at the west part of the area is not permanent on the two figures while those for east and center which are near mountains are very steady so that it can be easily thought that they are maintained by mountains. To examine this problem we decided to separate the CAPE into two parts, one computed from surface to 500 hPa ($\text{CAPE}_{1000-500}$) for which strong connection with topography of the area may be expected, and the second from 500 hPa to P_{top} around 200 hPa ($\text{CAPE}_{500-200}$). The results obtained for the mean fields for $\text{CAPE}_{1000-500}$ and $\text{CAPE}_{500-200}$ (not shown) show that the pattern are similar to the pattern of CAPE, there is a certain vertical homogeneity of the CAPE in the troposphere in this area. Next, we computed the correlation coefficients between rainfall and $\text{CAPE}_{1000-500}$ and $\text{CAPE}_{500-200}$, in the same conditions as for the CAPE.

For the 1000–500 hPa layer, Fig. 7a and b show the correlation coefficients with one day of time-lag and without time-lag, respectively. Fig. 7a is very similar to Fig. 6a, with r maximum values 0.36, 0.38, and 0.31 at the grid points (15°N , 22.5°E), (17.5°N , 7.5°E), and (15°N , 12.5°W), respectively. For the Fig. 7b, there is a very good coincidence with

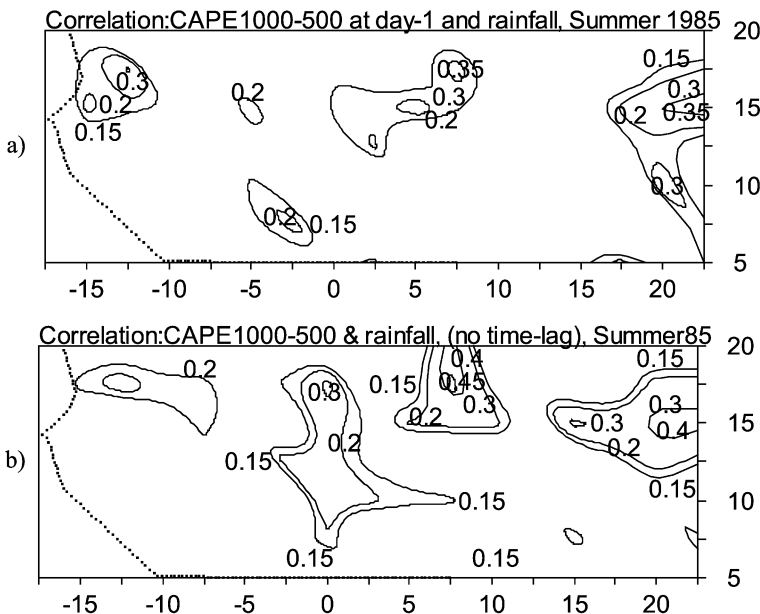


Fig. 7. Correlation between CAPE in the layer 1000–500 hPa and rainfall for Summer 1985; longitude (abscissa), latitude (ordinate) in degrees.

Fig. 6b, though the r maximum values are 0.39, 0.44, and 0.26 at the grid points (15°N, 20°E), (17.5°N, 7.5°E), and (15°N, 12.5°W), respectively.

For the layer 500–200 hPa, Fig. 8a and b displays the correlation coefficients with one day of time-lag and without time-lag, respectively. Fig. 8a and b are close to Fig. 6a and b, respectively, though r maximum values are 0.36, 0.38, and 0.27 at the grid points (15°N, 22.5°E), (17.5°N, 7.5°E), and (15°N, 12.5°W) for Fig. 8a, and 0.41, 0.47, and 0.18 at the grid points (15°N, 20.5°E), (17.5°N, 7.5°E), and (15°N, 12.5°W) for Fig. 8b.

Finally Fig. 7a for CAPE_{1000–500} and Fig. 8a for CAPE_{500–200} are systematically reproduced by Fig. 6a of CAPE, for 1 day time-lag, and Fig. 7b for CAPE_{1000–500} and Fig. 8b for CAPE_{500–200} by Fig. 6b of CAPE, with no time-lag. From these investigations, we can say that if the connection between the rainfall and the CAPE were due or amplified by the orography effects, one must admit that these effects remain strong or unchanged until the top level of the troposphere.

Furthermore, these coefficients of correlation do not exclusively show the dependencies between the two parameters, rainfall and CAPE. When we have $r \geq 0.2$ in a region, this does not systematically mean that rainfall and CAPE both have high values. We noted that, generally, on these figures, the correlation coefficients are very strong north of 12.5°N and become often maximum towards 15°N. Looking to the patterns of these two parameters, it is clear that the CAPE has its iso-line zero towards these latitudes where the rainfall daily mean value is very weak, under 2mm day⁻¹. Next, the two main cores of maximum

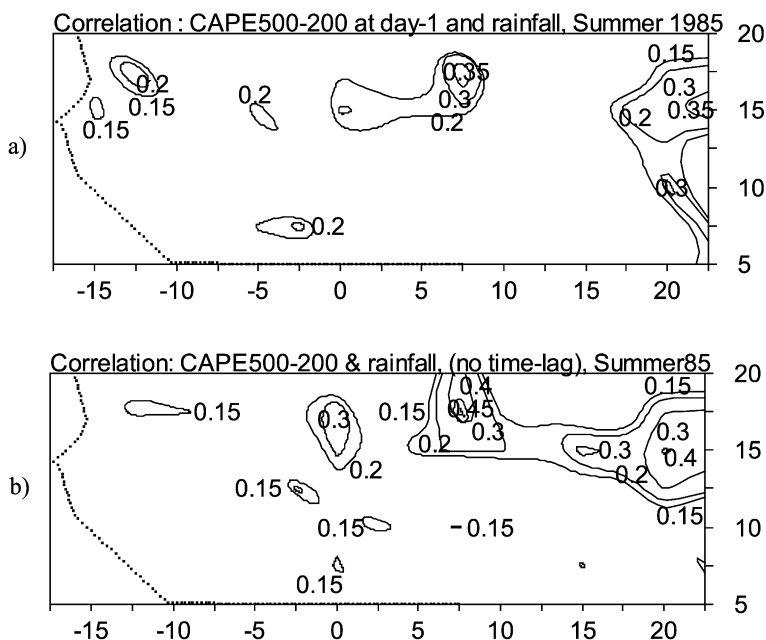


Fig. 8. Correlation between CAPE in the layer 500–200 hPa and rainfall for Summer 1985; longitude (abscissa), latitude (ordinate) in degrees.

coefficients of correlation, at the east and the center of the zone as it can be seen on Figs. 6a and b, 7a and b, 8a and b, are located near the mountains; the Hoggar and Tibesti mountains for the maximum towards the center and the Ethiopia and Darfur mountains for the maximum at the east. So, these fields of correlation coefficients seem to indicate the ITCZ and the orographic effects.

7. Discussion

7.1. Orographic effects

The pattern of CAPE that is observed on seasonal, menstrual, and decadal fields seems to be influenced by the geography of the studied area, in particular in the northern part of the equator. Kerry (1994), studying the observed characteristics of the precipitating convection, noted that the meteorological conditions that lead to vertical thermodynamic structures with large CAPE result from particular arrangements of geographical features.

In Fig. 9, adapted from Laurent et al. (1989), the main mountains appear above 1500 m of the northern part of the equator in the studied area. Some of these mountains are inside the zone of positive CAPE, while others surround the zone: at the east part of the zone, there is the Ethiopia mountain; the Darfur mountain is inside the zone in the north part, while Mont-cameroon mountain is in the south part. The Tibestibi and the Hoggar mountains limit the northern part of the zone of positive CAPE.

In order to discuss in the best conditions and also about the steadiness of the three regions of maximum inside the zone of positive CAPE, we referenced these three regions

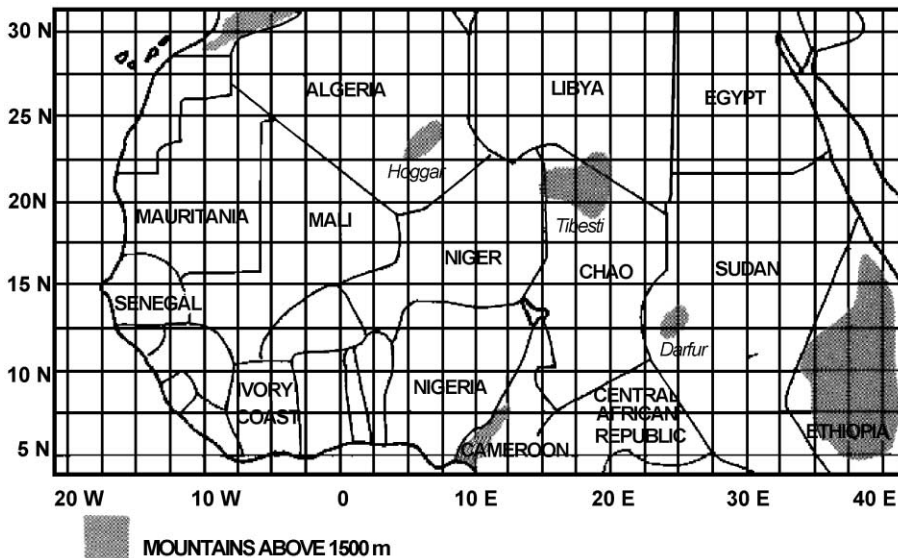


Fig. 9. Illustration of the location of the main mountains in the area of study (Adapted from Laurent et al. 1989).

as, I, II, and III by the band of longitudes 30°E – 20°E , 5°E – 5°W , and 10°W – 20°W , respectively.

The maximum in the region I, between 30°E and 20°E , is remarkably steady. This maximum is in general larger than the other two. As displayed on different figures, it appears on different time scales. The steadiness is probably linked to the orography since the maximum is located west of the mountains of Ethiopia or just east of the Darfur mountain (West Sudan), or between the Darfur and the Tibesti mountains (North Chad).

The maximum in region II (between 5°E and 5°W) is slightly smaller than the previous one. It seems to be not as steady as the maximum of region I. It is clearly marked on the mean field of summer, June and July; but it is not well distinguished in August and September. It seems to move westward towards the maximum of region III, so that these two maxima are sometimes confounded.

The western maximum is located in a surface thermal trough between the Libyan anticyclone to the east and the Azores anticyclone to the west. Reed et al. (1988) note this region lee of the Hoggar mountains in southeast of Algeria.

Among the three maxima, the one towards Greenwich meridian (region II) seems to be the most variable.

7.2. Waves and fluxes

Charney (1975), studying the dynamics of deserts and drought in the Sahel, noted that most of the world deserts occur in the subtropics and are associated with the descending branches of the tropical Hadley's circulation. This author seems to say that the deficit of energy appearing as what we saw in the Sahara desert, for example, can be filled by energy that is coming from the high atmospheric level and then transported downward by Hadley's cell in descending motion. This argument seems to be insufficient to explain how the energy deficit is completely filled in those areas.

Raschke and Bandeen (1970) made some investigations about the radiation balance of the planet Earth from radiation measurements of the satellite Nimbus-3 and showed that the net radiation at the top of the atmosphere is negative over the Sahara and Saudi Arabia deserts so that the radiation budget of Riehl and Malkus (1958) does not apply to northern Africa. According to Smith (1984), the mechanism of subsidence invoked to bring energy to the Sahara as described by Charney (1975) is not the only possible one. Therefore, there must be lower-level and mid-level horizontal transport over northern Africa to fill the energy deficit of the Sahara, and we suggest that the zone of positive CAPE, as we specified above, is the preferred area where this transport may occur. The southern equator energy deficit, as we observed in the studied area, must also benefit this horizontal energy transport southward from this zone. The waves observed in this region are in connection with convection and may play an important role in the horizontal northward and southward energy transport.

Cadet and Houston (1984) and Cadet and Nnoli (1987), using wind fields from ECMWF model analyses and specific humidity fields derived from TIROS-N moisture soundings, computed daily precipitable water over different areas of the tropical Atlantic and northern Africa, and daily water vapour fluxes across the equator for Summer 1979. They found major peaks at 3–5- and 6–9-day periods in the power spectrum of the

precipitable water and the fluxes series. These peaks may be connected to the fact that the two types of waves have important convective activities: Reed et al. (1977) showed that the African waves (3–5-day period) are in connection with convection, in particular towards the ITCZ around 10°N – 12°N in summer. Viltard et al. (1998) indicated that the 6–9-day waves are strongly modulated par convective activities towards 5°N – 7°N and 15°N – 20°N , on either side of the ITCZ mean position in summer. We suggest that these important wave convective activities are maintained with the help of the stock of CAPE in the band of latitude 0° – 20°N in the studied area. We also suggest that there is a meridional energy transport across the equator as for the fluxes, in order to fill the deficit of the energy that is observed in the southern part of the equator in the studied area during summer.

8. Summary and conclusion

In this study, we computed the convective available potential energy in northern Africa and tropical Atlantic in summer. The pattern of this parameter is quite steady and presents three main zones. The first one is located between the equator and 15°N – 20°N , with positive values of CAPE. In the second and the third zones located north of the band of latitudes 15°N – 20°N and south of the equator, respectively, CAPE has negative values. This pattern is conserved when CAPE is computed in the layers 1000–500 and 500–200 hPa. So, the CAPE seems to have a certain vertical homogeneity in the troposphere with a source of energy between the equator and a latitude inside the band 15°N – 20°N and a deficit of energy on either side of this source.

The pattern of the CAPE suggests possibilities of horizontal energy transport to fill the deficit observed in the Sahara and in the south of the equator. The waves can contribute to this energy transport. Monkam (1990) and De Felice et al. (1990) showed, using a compositing method, that the 6–9-day waves structure has a strong meridional wind component at about 5°N , equator-wards side; and about 20°N , pole-wards side. Next, Cadet and Houston (1984) and Cadet and Nnoli (1987) found major peaks at 3–5- and 6–9-day band periods in the spectra of precipitable water and water vapour fluxes across the equator, computed over different areas of the tropical Atlantic and northern Africa. We think that the transport of matters or fluxes by these waves is facilitated by the CAPE pattern with positive values (or energy source) in regions where these waves are very well developed.

We examined, in some details, the main tendencies of the CAPE pattern inside the first zone (CAPE >0, in general) and we compared them to the field of rainfall pattern. We noted that the CAPE pattern in this zone presents three regions of maximum values: west, center, and east of the zone. The east maximum and the maximum of the center seem to be connected with the orography effects. Between 15°N and 20°N , the CAPE distribution is characterised by its iso-line zero. This iso-line zero seems to define the north limit of the ITCZ. In fact, the position of the iso-line zero on the CAPE distribution fluctuates during summer as the position of the ITCZ so that this parameter can be also used as a parameter or an index to define the ITCZ position in northern Africa and tropical Atlantic.

The patterns of the rainfall and CAPE in this zone (5°N – 20°N) have very good similarity. When the rainfall is very weak ($<2\text{ mm day}^{-1}$) towards 12.5°N – 15°N , the CAPE tends to zero. The rainfall pattern presents, in general, high values towards Guinea

and around Lake Chad. These regions are not very far from the maximum values of CAPE observed in different figures.

The fields of correlation coefficients between the two parameters show that the rainfall and the CAPE are very well correlated around the ITCZ and towards some mountains. So, the high values of the correlation coefficients seem to indicate that, each of these two parameters is influenced by the ITCZ effects and by the orography effects. We suggest that the CAPE may be studied in connection with some dynamic effects of this region.

References

- Balaji, V., Redelsperger, J.L., 1996. Sub-gridscale effects in mesoscale deep convection: initiation, organization and turbulence. *Atmos. Res.* 40, 339–381.
- Cadet, D.L., Houston, S.H., 1984. Precipitable water over West Africa and eastern Central Atlantic ocean during summer 1979. *J. Meteorol. Soc. Japan* 62, 761–774.
- Cadet, D.L., Nnoli, N.O., 1987. Water vapour transport over West Africa and the Atlantic ocean during summer 1979. *Q. J. R. Meteorol. Soc.* 113, 581–602.
- Charney, J.G., 1975. Dynamics of deserts and drought in the Sahel. *Q. J. R. Meteorol. Soc.* 101, 193–202.
- De Felice, P., Viltard, A., Monkam, D., Ouss, C., 1990. Characteristics of North African 6–9-day waves during summer 1981. *Mon. Weather Rev.* 118, 2624–2633.
- Duvel, J.P., 1989. Convection over tropical Africa and Atlantic ocean during northern summer. Part I: interannual and diurnal variations. *Mon. Weather Rev.* 117, 2782–2799.
- Duvel, J.P., 1990. Convection over tropical Africa and Atlantic ocean during northern summer. Part II: modulations by easterly waves. *Mon. Weather Rev.* 118, 1855–1868.
- Fontaine, B., Janicot, S., Roucou, P., 1999. Coupled ocean-atmosphere surface variability and its climate impacts in the tropical Atlantic region. *Clim. Dyn.* 15, 451–473.
- Holton, J.R., 1992. A introduction to dynamic meteorology. *International Geophysics Series*, vol. 48. Academic press, London, 511 pp.
- Kerry, A.E., 1994. Atmospheric convection. Oxford Univ. Press, New York, 580 pp.
- Laurent, H., Viltard, A., de Felice, P., 1989. Performance evaluation and local adaptation of the ECMWF system forecasts over Northern Africa for summer 1985. *Mon. Weather Rev.* 117, 1999–2009.
- Moncrieff, M.W., Miller, M.J., 1976. The dynamics and simulations of tropical cumulonimbus and squall lines. *Q. J. R. Meteorol. Soc.* 432, 373–394.
- Monkam, D., 1990. Ondes troposphériques d'échelle synoptique en Afrique: caractérisation cinématique, structure et étude spatio-temporelle et comparative de deux systèmes d'ondes d'été aux moyens de données d'analyse. Thesis, University of Paris 6, 212 pp. (in French).
- Peppler, R.A., Lamb, P.J., 1989. Tropospheric static stability and central north american growing season rainfall. *Bull. Am. Meteorol. Soc.* 117, 1156–1180.
- Raschke, E., Bandeen, W.R., 1970. The radiation Balance of the planet Earth from radiation measurements of the satellite Nimbus-3. *J. Appl. Meteorol.* 9, 215–238.
- Reed, R.J., Norquist, D.C., Recker, E.E., 1977. The structure and properties of African wave disturbances as observed during phase III of GATE data. *Mon. Weather Rev.* 105, 317–333.
- Reed, R.J., Klinder, E., Hollingsworth, A., 1988. The structure and characteristics of African easterly wave disturbances as determined from ECMWF operational analysis forecast system. *Meteor. Atmos. Phys.* 38, 22–33.
- Riehl, H., Malkus, J.S., 1958. On the heat balance in the equatorial trough zone. *Geophysica* 6, 503–538.
- Rotunno, R., Klemp, J.B., 1982. The influence of shear-induced pressure gradient on the thunderstorm motion. *Mon. Weather Rev.* 110, 136–151.
- Showalter, A.K., 1953. A stability index for thunderstorm forecasting. *Bull. Am. Meteorol. Soc.* 34, 250–252.
- Smith, E.A., 1984. Radiative forcing of the southwest summer monsoon: A satellite perspective. *Atmospheric science paper No. 383*, 520 pp. [Available from Department of Atmospheric Science, Colorado State University, Fort Collins, Colorado 80523.]

- Sow, C.S., 1997. Diurnal rainfall in Senegal. *Secheresse* 8, 157–162.
- Viltard, A., De Felice, P., Oubuih, J., 1998. Rainfall and the 6–9-day wave-like disturbance patterns in West Africa during summer 1989. *Meteorol. Atmos. Phys.* 66, 229–234.
- Weisman, M.L., Klemp, J.B., 1982. The dependence of numerically simulated convective storms on vertical wind shear and the buoyancy. *Mon. Weather Rev.* 110, 504–520.